Lifetime imaging of radiative and non-radiative fluorescence decays on nanoplasmonic surface

Manas Ranjan Gartia, John P. Eichorst, Robert M. Clegg, and G. Logan Liu

Citation: Applied Physics Letters **101**, 023118 (2012); doi: 10.1063/1.4736575
View online: http://dx.doi.org/10.1063/1.4736575
View Table of Contents: http://scitation.aip.org/content/aip/journal/apl/101/2?ver=pdfcov
Published by the AIP Publishing

Lifetime imaging of radiative and non-radiative fluorescence decays on nanoplasmonic surface

Manas Ranjan Gartia,[1,a)] John P. Eichorst,[2,3,a)] Robert M. Clegg,[3,b)] and G. Logan Liu[4,c)]
[1]*Department of Nuclear, Plasma and Radiological Engineering, University of Illinois at Urbana-Champaign, Urbana, Illinois 61801, USA*
[2]*Center of Biophysics and Computational Biology, University of Illinois at Urbana-Champaign, Urbana, Illinois 61801, USA*
[3]*Department of Physics and Department of Biochemistry, University of Illinois at Urbana-Champaign, Urbana, Illinois 61801, USA*
[4]*Department of Electrical and Computer Engineering, University of Illinois at Urbana-Champaign, Urbana, Illinois 61801, USA and Department of Bioengineering, University of Illinois at Urbana-Champaign, Urbana, Illinois 61801, USA*

(Received 21 February 2012; accepted 25 June 2012; published online 13 July 2012)

We report the fluorescence lifetime imaging and quantum yield measurement of five different fluorescence dyes spanning different quantum yield and excitation wavelength ranges in solution as well as on irregular nanoplasmonic substrate surface. Due to a distribution of dye molecules at random distances and orientation to the metal nanoplasmonic structure, the dyes showed multi-component lifetime decays on the surface. We have simulated the distribution of lifetime on the surface based on fractional intensity relative to steady-state value and derived an average lifetime with species fraction. From the quantum yield and fluorescence lifetime measurements we calculated the modified radiative and non-radiative decay rates for the dyes due to energy coupling on the substrate. We measured up to 100 fold fluorescence enhancement on nanoplasmonic substrate, and all molecule fluorescence showed not only considerably higher radiative decay rate but also higher non-radiative decay rate. © *2012 American Institute of Physics*.
[http://dx.doi.org/10.1063/1.4736575]

For a spontaneous emission process, the rate of transition from an excited state k to another state l can be calculated using Fermi's golden rule, which can be written as $w_{kl} = \frac{2\pi}{\hbar}\rho\left(\frac{E_k - E_l}{h}\right)|M_{kl}|^2$. M_{kl} is the transition matrix element between the excited and lower energy state. The value of M_{kl} is determined by the wavefunctions associated with those levels. $\rho\left(\frac{E_k - E_l}{h}\right) = \rho(\nu)$ is the density of states at the transition frequency, $\nu = \frac{E_k - E_l}{h}$; $\rho(\nu)$ is also known as the photonic mode density (PMD)—the number of photon modes available at the frequency ν.[1] Hence, the rate of fluorescence emission can be influenced by changing $\rho(\nu)$.[2] Increasing PMD leads to faster decay rates.[3] For instance, a fluorophore close to a metal nanoparticle or surface can experience an increase in the PMD available for spontaneous emission at a particular frequency, ν, shortening the natural radiative lifetime. In addition, the proximity of a metal particle or surface can increase the magnitude of the impinging electromagnetic field surrounding a fluorophore, thereby increasing the rate of absorption (or stimulated emission). The latter also increases the measured fluorescence intensity by increasing the rate of forming excited molecules for a certain impinging light intensity.[1,3] This modification in the emission properties of a fluorophore in close proximity to metals is known as surface enhanced fluorescence (SEF)[4] or metal enhanced fluorescence (MEF). It can be used to increase the signal level when imaging fluorescent molecules. As a result the long time stability of dyes is increased because the rate of leaving the excited state is faster (lowering the relative probability of going to the triplet state, decreasing the rate of photolysis). In addition, the limit of detectable concentrations for many fluorescent materials will become lower.[5,6]

The enhancement of fluorescence due to the augmentation of electric field near a metal nanostructure is attributed to two different mechanisms: (1) an increase in the excitation field due to the reflection of the excitation light and also redirection of the emitted light by the metal surface toward the objective lens increasing the collection efficiency (mirror effect)[7] and (2) surface plasmon resonance at the surface of the metal nanostructure brought about by the electric field of the incident light interacting with the free electrons on the surface of the metal.[6] If the Frohlich condition is met, maximum polarizability and resonance will occur resulting in the amplification of the near field both inside and outside of the nanostructure.[6] The enhanced excitation of the fluorescent molecule is due to the amplification of near field outside of the nanostructure.[8,9] The degree of interaction (transfer of energy) between the metal and fluorophore depends strongly on the distance between the dye and the surface as well as the overlap between the scattering spectra of the surfaces and the absorption/emission spectra of fluorophore (for better enhancement due to surface plasmon resonance).[10] When the fluorophore is too close to the metal surfaces (<5 nm) a damping of the oscillation of the molecule's dipole may occur that generally leads to fluorescence quenching (usually this has a d^{-3} dependence where d is the distance between the metal surface and dye molecule).[11]

[a)]M. R. Gartia and J. P. Eichorst contributed equally to this work.
[b)]Electronic mail: rclegg@illinois.edu.
[c)]Electronic mail: loganliu@illinois.edu.

Another issue of the emission process is whether the observed fluorescence is emitted by the fluorophore or by the surface plasmon. In the process known as radiative decay engineering (RDE), the fluorophore resonantly interacts with the metal nanostructure resulting in enhanced fluorescence being emitted by the fluorophore itself.[12] Observation of directional emission from a fluorophore at short distances prompted the idea of surface plasmon coupled emission (SPCE), where non-radiative energy transfer occurs from an excited fluorophore to surface plasmon electrons in the metallic nanostructure. Under certain boundary conditions, radiation is thought to be emitted by surface plasmons.[13]

Although the coupling between fluorophores and nanostructures with simple geometries is relatively well understood, the fluorescence emission patterns of more complex nanostructures, such as percolated or roughened metallic thin films, are under active investigation.[4] For example, on an irregular corrugated metallic structure, the surface plasmon wave vector behaves differently than the Bragg-scattered bound-mode features on a grating. For a grating with periodicity a, the surface plasmon wave vector is $k'_{sp} = k_{sp} \pm ng_B = k_{sp} \pm n(2\pi/a)$, where k_{sp} is surface plasmon (SP) wave vector at the metal-air interface and g_B is the grating or Bragg wave vector.[4] The periodic grating structure imposes a very strict condition on photon momentum for coupling to SPs (hence usually both coupling as well as emission can only occur at certain angles), whereas a random nanostructure relaxes this condition allowing broadly distributed angles for coupling to SPs. In addition, the randomness of the structure leads to the possibility of strong constructive interference of SPs at certain locations which will give rise to very high electromagnetic fields ("hot spots"), also known as Anderson localization.[14,15] Hence, the resulting electric field associated with SPs is expected to be more intense for the case of random metallic nanostructure as compared to smooth metal surface or glass substrate. This provides additional enhancement for the excitation field and consequently greater fluorescence enhancement.

Determining different decay rate constants (radiative and non-radiative pathways of deactivation) requires measuring both the lifetimes and quantum yields on the surface. Although both the lifetime and the quantum yield of a fluorophore conjugated to nanoparticles have been measured,[16–19] only the lifetime of the fluorophore has been measured on the surface of substrate.[20–22] This is because the quantum yield of the fluorophore is generally measured by using the methods of Williams and Winfield,[23] where the absorbance and emission of the dyes are compared with that of a known reference compound. However, when the samples significantly scatter light, the photons scattered by the structure will be further absorbed by the dyes and will give rise to additional light emission leading to overestimation of the quantum yield rendering the previously described method invalid.[24] Therefore, we have measured the fluorescence lifetime (with fluorescence lifetime imaging microscopy (FLIM)) and the quantum yield of five different dyes free in solution as well as on irregular nanoplasmonic substrates. We have chosen the dyes to span different quantum yield ranges (low, medium and high) and also different excitation wavelength ranges (blue, green).

Figure 1(a) shows the bright field image of the prepared nanoplasmonic substrate. After a photolithographic step to prepare the square pattern, the nanopillar structures are created inside the square area using a mask-less ICP-RIE process (inductively coupled plasma-reactive ion etching) with a mixture of HBr and O_2 gases. Figure 1(b) presents the angular view (30°) SEM image of the nanostructure region after metallization (80 nm Ag) to render the structure with plasmonic property. For all the experiments 5 μl of 10 μM dyes (which typically makes a drop of about 3 mm diameter) are dropped on to the surface covering several square patterns. The FLIM system used is shown in Fig. 1(c). Since the modulation of the lifetime is nonlinearly dependent on the distance from the metal surface[22] and fluorophores are randomly distributed on the metallic nanostructure, we expect a distribution of lifetime component on the nanoplasmonic substrate instead of a single lifetime component. Figure 1(d) shows an example of exponential decays for two different distances "d" from the metal nanostructure surface. The lifetime of single fluorophore in direct contact (d = 0) to the metal surface is zero and increases non-linearly with increasing distance from the metal surface reaching asymptotically the free fluorophore (without metal surface) lifetime.[22] The polar plot is shown in Fig. 1(e) where the positions of lifetimes for free solution and those on nanoplasmonic substrate are shown. The data points on the polar plot, in this case due to a multi-component decay kinetics of fluorophore on nanoplasmonic surface, lie inside the semicircle of the polar plot

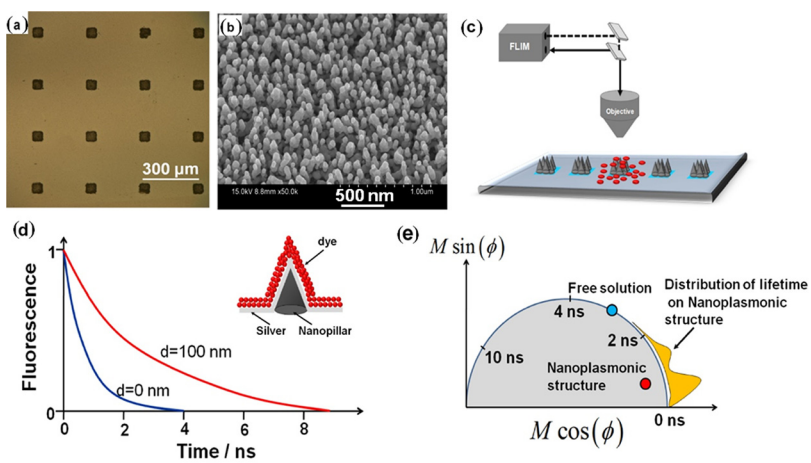

FIG. 1. (a) Bright field image of the nanoplasmonic substrate. The square region contains the nanostructure. (b) Angular (30°) SEM image of the nanostructure region after 80 nm Ag deposition. (c) Schematic diagram of FLIM experimental set-up. (d) Schematic of lifetime distribution of dyes ($I(t) = \sum_{i=1}^{n} \alpha_i \exp(-t/\tau_i)$, α_i are the amplitudes and τ_i are the lifetimes) on nanoplasmonic substrate. Here, "d" is the distance of the dye from the nanoplasmonic substrate. (e) Sketch of polar plot and lifetime distribution for the population of dyes on nanoplasmonic substrate. Here, ϕ is the phase corresponding to lifetime component.

as shown in Fig. 1(e). Except for emission of a molecule that is excited via an excited state reaction, polar plot points due to a distribution of lifetime values will always lie inside this semi-circle.

Five different dyes, Rhodamine6G or R6G ($\lambda_{ex} = 532$ nm), Fluorescein ($\lambda_{ex} = 440$ nm), Acridine Orange ($\lambda_{ex} = 440$ nm), Rhodamine-B ($\lambda_{ex} = 532$ nm), and Eosin-Y ($\lambda_{ex} = 532$ nm) are chosen to cover different quantum yields and ranges of excitation wavelength (λ_{ex}). The quantum yields for the dyes are determined experimentally using R6G as a reference with a known quantum yield $Q_R \sim 0.90$ in aqueous media.[25] The quantum yield was calculated as[23] $Q = Q_R \frac{I}{I_R}\frac{OD_R}{OD}\frac{n^2}{n_R^2}$, where Q is the quantum yield, I is the fluorescence intensity integrated over the wavelengths of emission, OD is the optical density, and n is the refractive index; the suffix R indicates the reference (R6G). Figure 2(a) shows a typical absorbance and fluorescence measurement for Rhodamine-B (Rh-B) used for a quantum yield calculation (results for other dyes can be found in supporting information). The phase delay and modulation ratio of the dyes free in solution are detected using a frequency-domain FLIM system. In this paper, the modulation ratio and phase delay are projected as coordinates on the polar plot.[26,27] The measured lifetime of the dyes are reported in Table I and are comparable to those reported in the literature. Using the quantum yield and lifetime data, the radiative and nonradiative decay rates of the fluorophore in free solution were calculated as: $\Gamma_0 = Q_0/\tau_0$ and $(k_{nr})_0 = \frac{1}{\tau_0} - \Gamma$, the results are shown in Table I. We modified Nikon E600FN microscope set up to measure the quantum yield of dyes on the nanoplasmonic substrate. The camera of the microscope was replaced by a spectrometer (B&W Tek Inc.), and the emission filter was removed to register both the excitation as well as emission spectra during the experiment.

The absorption and emission spectra of the Rh-B on the nanoplasmonic substrate are shown in Fig. 2(b). The emission spectrum of the surface without dye (black curve) is a measure of the difference between scattering intensity and absorption intensity by the surface $(I_{scat} - I_{abs,nanopillar})$. The spectrum for surfaces with the dye (red curve) is due to the combination of absorption and emission spectrum from the dye. The absorption part of spectrum is a result of scattering from the surface and dye lowered by absorption by the surface and by the dye, $(I_{scat} + I_{scat,dye} - I_{abs,nanopillar} - I_{abs,dye})$. The emission spectrum $(I_{em,dye})$ describes the fluorescence of the dye on the surface. The difference between integrated area of absorption spectra with and without the dye corresponds to the relative intensity of absorption by the dye on the surface $(I_{abs,dye})$ neglecting the scattering from the dye. The integrated area of the emission spectrum is a measure of total emission intensity by the dye while on the surface $(I_{em,dye})$. Hence, we can estimate the quantum yield of dye on the surface from the ratio of emission intensity of the dye to the absorption intensity of the dye $(Q_{\mathrm{mod}} = I_{em,dye}/I_{abs,dye})$.

Figure 2(c) shows the fluorescence intensity image of Rh-B on the nanoplasmonic substrate. The intensity showed typical spatial heterogeneity with several brighter spots due to "hot spots" of the substrate. The phase-sensitive images of frequency domain FLIM were used to calculate the apparent phase (τ_Φ) and modulation (τ_M) lifetimes. Also, the polar plot coordinates for the Rh-B FLIM data on the nanopillar substrate are shown in Fig. 2(d); the data clearly moved toward the region of lower lifetimes on the polar plot as compared to the dye free in solution. Figure 2(e) compares the fluorescence spectroscopy result for Rh-B on nanoplasmonic and glass substrate. The ratio between integrated fluorescence intensity of Rh-B on nanoplasmonic substrate and that on glass substrate provides an estimate for the fluorescence enhancement (far field) experienced by the dye. The fluorescence enhancement for Rh-B was measured to be 5.13 on the nanoplasmonic substrate. The maximum enhancement factor observed for various dyes are reported in Table I. The signal enhancement can be explained by the radiative conversion of energy transferred from the dyes to SPs. On glass substrate, the energy transferred from the dyes only dissipates in the glass and cannot be detected. On the other hand, roughened metal nanostructure enhances the light scattering and allow the efficient coupling between light and SPs. Thus, the energy transferred from the dye to metal surface can be recovered by the re-radiation by the SPs.[28]

Figures 3(a) and 3(b) shows the spatial distribution of the effective lifetimes derived from the measured phase delay τ_Φ and modulation ratio τ_M from the nanoplasmonic substrate, respectively. The corresponding histograms of phase delay for free solution and dye on nanoplasmonic substrate are shown in Figs. 3(c) and 3(d). For a multiexponential decay process, the apparent phase lifetime is shorter than the apparent

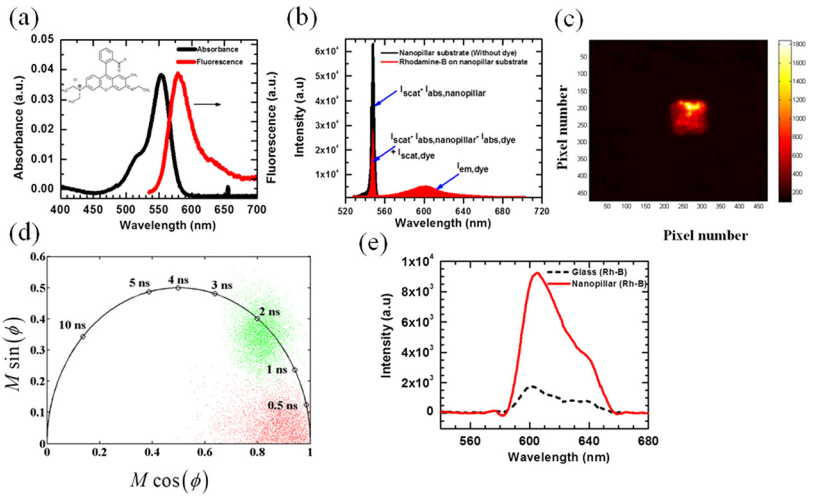

FIG. 2. (a) Absorbance and fluorescence spectra for Rh-B in aqueous solution. (b) Emission spectra of the Rh-B on the nanoplasmonic substrate. (c) Fluorescence intensity image of Rh-B on the nanoplasmonic substrate. The increase is fluorescence intensity on the nanoplasmonic substrate (square region) compared to surrounding smooth metal (Ag) region is apparent. (d) Polar plot representation of lifetime for Rh-B in free solution (Petri Dish) and on nanoplasmonic substrate (Nanopillar). (e) Comparison of the fluorescence spectroscopy result for Rh-B on nanoplasmonic substrate and on glass substrate.

TABLE I. Fluorescence lifetime analysis: I_{nano}, fluorescence intensity on the nanoplasmonic structure; I_{glass}, fluorescence intensity on glass substrate; *EF*, fluorescence enhancement factor.

Fluorophore	τ_0 (ns)	Q_0	Γ_0 (s^{-1})	$(k_{nr})_0$ (s^{-1})	τ_{mod} (ns)	Q_{mod}	Γ_{mod} (s^{-1})	$(k_{nr})_{mod}$ (s^{-1})	*EF* (I_{nano}/I_{glass})
R6G	4.11	0.90	2.19×10^8	2.43×10^7	0.219	0.992	4.52×10^9	3.65×10^7	20.5
Fluorescein	4.38	0.95	2.17×10^8	1.14×10^7	0.182	0.991	5.45×10^9	4.84×10^7	100
Acridine Orange	2.04	0.29	1.42×10^8	3.48×10^8	0.443	0.753	1.70×10^9	5.58×10^8	8.34
Rhodamine-B	1.67	0.41	2.46×10^8	3.53×10^8	0.104	0.857	8.20×10^9	1.37×10^9	5.13
Eosin-Y	1.31	0.32	2.42×10^8	5.21×10^8	0.277	0.845	3.05×10^9	5.60×10^8	4.3

modulation lifetime.[29] The lifetimes determined from both the phase delay and modulation ratio were found to be reduced on the nanoplasmonic substrate. The observation of $\tau_\Phi < \tau_M$ (shown in supplementary figures) is consistent with a multiexponential decay on the nanoplasmonic substrate.

The data collected on the FLIM system was analyzed with a set of simulations on the polar plot. All simulations performed on the polar plot were based on the analysis of fractional intensities on the polar plot. When the phase delay (ϕ_{TOT}) and modulation ratio (M_{TOT}) are projected as a polar coordinate, variations of the fractional intensities (α) in the fluorescent species can easily be monitored. In other words, for a complicated fluorescent sample, the contribution of each constituent fluorophore's emission to the measured steady-state intensity (α_i) determines the position of the polar coordinate of the sample relative to the polar coordinates of the constituent contributing fluorescence species (i) with the following equations: $x = \sum_i \alpha_i M_i \cos(\phi_i) = M_{TOT} \cos(\phi_{TOT})$, $y = \sum_i \alpha_i M_i \sin(\phi_i) = M_{TOT} \sin(\phi_{TOT})$.

In the above equations, (M_i) is the modulation factor associated with lifetime component (i) and (ϕ_i) is phase corresponding to lifetime component (i). $M_i = \frac{1}{\sqrt{1+(\omega\tau_i)^2}}$. $\phi_i = tan^{-1}(\omega\tau_i)$. The resulting polar coordinate of a sample characterized by many single lifetimes must lie inside the universal semi-circle.[26,27] The extent to which the polar coordinate generated by a large distribution of lifetimes lies inside the semi-circle depends on the intensity weighting of the fractional intensities of the single lifetimes in the distribution. A graphical representation of such distributions is presented on the polar plot (Fig. 4(a)). In this work, polar plot data were simulated as a set of two Gaussian lifetime distributions (Fig. 4(b)). As shown, there was a definite decrease in lifetime accompanied by an increase in fractional intensity, consistent with metal-enhanced fluorescence (Fig. 4(a)). The measured polar coordinates for the nanopillar, smooth silver film, and background were used in the simulations (Fig. 4(c)).

The measured quantum yield of Rh-B on the nanopillar surface was 86%, which was a 2-fold increase from the value in solution. Generally, the quantum yield of a fluorophore reflects a competition between radiative and non-radiative decay processes, and the natural radiative rate does not change.[3] The lifetime of a fluorophore is the average time an ensemble of molecules remains in the excited state; therefore, the lifetime is influenced by all the de-excitation pathways—fluorescence, dynamic quenching, non-radiative decay, energy transfer, etc.—that are available for exiting the excited state. The shortened lifetime on the surface can be explained by the fact that the proximity of the metal provides an additional pathway of de-excitation, which increases the rate at which the molecule will leave the excited state.

The modified decay rates on the surface are calculated from the quantum yield and lifetime measurement as $\Gamma_{mod} = Q_{mod}/\tau_{mod}$ and $(k_{nr})_{mod} = \frac{1}{\tau_{mod}} - \Gamma_{mod}$. The modified decay rates are reported in Table I. The increased quantum yield on the surface is primarily due to increase in radiative decay rate for Rh-B. For the high quantum yield dyes in free solution, the ratio of radiative to non-radiative decay rates (r) are usually greater than 1 (e.g., $r_{Fluorescein} = 19.0$, $r_{R6G} = 9.0$). The ratios for other dyes in free solution with lower quantum yield are less than 1 ($r_{AO} = 0.41$, $r_{EY} = 0.46$, $r_{Rh-B} = 0.70$). However, on nanostructure the ratio of radiative to non-radiative decay rates is always greater than 1 for all the dyes. The largest change in quantum yield was found for Eosin-Y where the quantum yield increased by 2.67 fold from that in free solution dye. However, the fluorescence enhancement for Eosin-Y measured on the nanosctructure as compared to glass substrate was the lowest. The variation of fluorescence enhancement is highly non-linear and did not necessarily follow any discernable trend. In general, the enhancement decreases with increasing non-radiative decay rate.[30]

In conclusion, we measured the steady-state fluorescence to determine the quantum yields and we used frequency-domain FLIM to determine the time-dependent decay of five

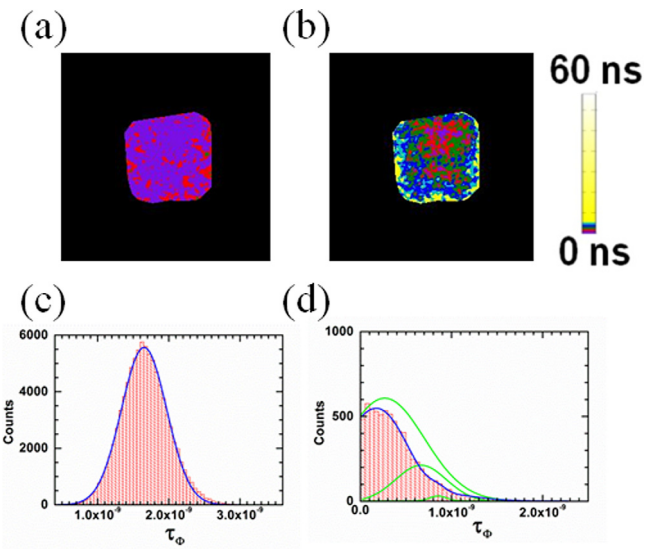

FIG. 3. (a) Fluorescence phase lifetime image of Rh-B on nanoplasmonic substrate. (b) Fluorescence modulation lifetime images of Rh-B on the nanoplasmonic substrate. (c) Histogram for lifetime measurement of Rh-B in free solution. (d) Histogram for lifetime measurement of Rh-B on nanoplasmonic substrate.

(a)

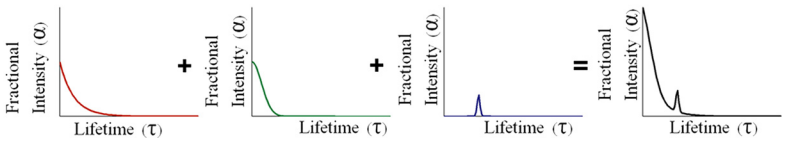

(b)

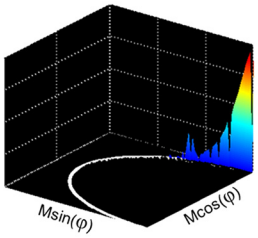

(c)

	Nanopillar (x,y)	Smoothsilver (x,y)	Background Nanopillar (x,y)
Rhodamine B	(0.9138,0.03438)	(0.8212,0.1793)	(0.2638,0.06805)
Fluorescein	(0.8678,.0596)	(0.8171,0.3563)	(0.4214,0.1277)
Rhodamine 6G	(0.9142,.05354)	(0.8636,0.06757)	(0.575,.05059)

FIG. 4. Descriptions of life time simulations. (a) The principle components of the distributions of lifetimes are displayed as a function of fractional intensities. An exponentially decreasing set of lifetimes as function of fractional intensities (far left panel) is combined with Gaussian distributions (middle two panels) each representing the smooth-silver and nanopillar separately to determine the final distribution (far right panel). (b) A three dimensional view of the general profile of the simulated distributions is presented on the polar plot. The color hue represents an increasing fractional intensity (blue to red). (c) These measured polar coordinates were applied to the simulations to establish the locations of the nanopillar and smooth silver film distributions. Background was factored in separately.

different dyes in free solution as well as on irregular nanoplasmonic substrate. We obtained a surface fluorescence enhancement of ~100 folds for fluorescein on the nanoplasmonic substrate compared to that on glass. The results provide a way to determine the quantum yield of dyes on highly scattering surfaces and analyze lifetime data for the population of fluorophores randomly distributed on a nanoplasmonic substrate.

[1]W. L. Barnes, J. Mod. Opt. **45**, 661 (1998).
[2]E. M. Purcell, Phys. Rev. **69**, 681 (1946).
[3]C. D. Geddes and J. R. Lakowicz, J. Fluoresc. **12**, 121 (2002).
[4]E. Fort and S. Gresillon, J. Phys. D: Appl. Phys. **41**, 013001 (2008).
[5]J. Fu, B. Park, G. Siragusa, L. Jones, R. Tripp, Y. Zhao, and Y.-J. Cho, Nanotechnology **19**, 155502 (2008).
[6]S.-H. Guo, J. J. Heetderks, H.-C. Kan, and R. J. Phaneuf, Opt. Express **16**, 18417 (2008).
[7]J. Kummerlen, A. Leitner, H. Brunner, F. R. Aussenegg, and A. Wokaun, Mol. Phys. **80**, 1031 (1993).
[8]M. Moskovits, Rev. Mod. Phys. **57**, 783 (1985).
[9]P. Anger, P. Bharadwaj, and L. Novotny, Phys. Rev. Lett. **96**, 113002 (2006).
[10]K. Lee, L. D. Hahn, W. W. Yuen, H. Vlamakis, R. Kolter, and D. J. Mooney, Adv. Mater. **23**, H101 (2011).
[11]A. Campion, A. R. Gallo, C. B. Harris, H. J. Robota, and P. M. Whitmore, Chem. Phys. Lett. **73**, 447 (1980).
[12]J. R. Lakowicz, Anal. Biochem. **298**, 1 (2001).
[13]J. R. Lakowicz, Anal. Biochem. **337**, 171 (2005).
[14]D. S. Wiersma, P. Bartolini, A. Lagendijk, and R. Righini, Nature (London) **390**, 671 (1997).
[15]K. Arya, Z. B. Su, and J. L. Birman, Phys. Rev. Lett. **54**, 1559 (1985).
[16]R. Bardhan, N. K. Grady, J. R. Cole, A. Joshi, and N. J. Halas, ACS Nano **3**, 744 (2009).
[17]F. E. Hernandez, S. J. Yu, M. Garcia, and A. D. Campiglia, J. Phys. Chem. B **109**, 9499 (2005).
[18]M. E. Sanborn, B. K. Connolly, K. Gurunathan, and M. Levitus, J. Phys. Chem. B **111**, 11064 (2007).
[19]H. S. Muddana, T. T. Morgan, J. H. Adair, and P. J. Butler, Nano Lett. **9**, 1559 (2009).
[20]J. R. Lakowicz, Y. B. Shen, S. D'Auria, J. Malicka, J. Y. Fang, Z. Gryczynski, and I. Gryczynski, Anal. Biochem. **301**, 261 (2002).
[21]Y. Zhang, K. Aslan, M. J. R. Previte, and C. D. Geddes, Appl. Phys. Lett. **90**, 053107 (2007).
[22]M. Berndt, M. Lorenz, J. Enderlein, and S. Diez, Nano Lett. **10**, 1497 (2010).
[23]A. T. R. Williams, S. A. Winfield, and J. N. Miller, Analyst **108**, 1067 (1983).
[24]M. Martini, M. Montagna, M. Ou, O. Tillement, S. Roux, and P. Perriat, J. Appl. Phys. **106**, 094304 (2009).
[25]D. Magde, R. Wong, and P. G. Seybold, Photochem. Photobiol. **75**, 327 (2002).
[26]G. I. Redford and R. M. Clegg, J. Fluoresc. **15**, 805 (2005).
[27]S. Matsubara, Y. C. Chen, R. Caliandro, Govindjee, and R. M. Clegg, J. Photochem. Photobiol. B: Biol. **104**, 271 (2011).
[28]E. Le Moal, S. L. Fort, M. C. Potier, and E. Fort, Nanotechnology **20**, 225502 (2009).
[29]S. Murata, P. Herman, H. J. Lin, and J. R. Lakowicz, Cytometry **41**, 178 (2000).
[30]See supplemental material at http://dx.doi.org/10.1063/1.4736575 for the polar plot, absorbance and fluorescence spectroscopy, literature data for the lifetime of dyes as well as statistical distribution and correlation of phase and modulus lifetime for all five dyes.